

DOI: 10.1007/s11430-006-8047-2

## Seasonal variation of carbon exchange of typical forest ecosystems along the eastern forest transect in China

ZHANG Leiming<sup>1,5</sup>, YU Guirui<sup>1</sup>, SUN Xiaomin<sup>1</sup>, WEN Xuefa<sup>1</sup>, REN Chuanyou<sup>1</sup>, SONG Xia<sup>1</sup>, LIU Yunfen<sup>1</sup>, GUAN Dexin<sup>2</sup>, YAN Junhua<sup>3</sup> & ZHANG Yiping<sup>4</sup>

1. Synthesis Center of Chinese Ecosystem Research Network (CERN), Institute of Geographic Sciences and Natural Resources Research, Chinese Academy of Sciences, Beijing 100101, China;

2. Institute of Applied Ecology, Chinese Academy of Sciences, Shenyang 110016, China;

3. South China Institute of Botany, Chinese Academy of Sciences, Guangzhou 510650, China;

4. Xishuangbanna Tropical Botanical Garden, Chinese Academy of Sciences, Kunming 650223, China;

5. Graduate University of Chinese Academy of Sciences, Beijing 100049, China

Correspondence should be addressed to Yu Guirui (email: yugr@igsnrr.ac.cn)

Received October 27, 2005; accepted March 10, 2006

**Abstract** The long-term and continuous carbon fluxes of Changbaishan temperate mixed forest (CBS), Qianyanzhou subtropical evergreen coniferous forest (QYZ), Dinghushan subtropical evergreen mixed forest (DHS) and Xishuangbanna tropical rainforest (XSBN) have been measured with eddy covariance techniques. In 2003, different responses of carbon exchange to the environment appeared across the four ecosystems. At CBS, the carbon exchange was mainly determined by radiation and temperature. 0°C and 10°C were two important temperature thresholds; the former determined the length of the growing season and the latter affected the magnitude of carbon exchange. The maximum net ecosystem exchange ( $N_{EE}$ ) of CBS occurred in early summer because maximum ecosystem photosynthesis ( $G_{PP}$ ) occurred earlier than maximum ecosystem respiration ( $R_0$ ). During summer, QYZ experienced severe drought and  $N_{EE}$  decreased significantly mainly as a result of the depression of  $G_{PP}$ . At DHS and XSBN,  $N_{EE}$  was higher in the drought season than the wet season, especially the conversion between carbon sink and source occurring during the transition season at XSBN. During the wet season, increased fog and humid weather resulted from the plentiful rainfall, the ecosystem  $G_{PP}$  was depressed. The  $Q_{10}$  and annual respiration of XSBN were the highest among the four ecosystems, while the average daily respiration of CBS during the growing season was the highest. Annual  $N_{EE}$  of CBS, QYZ, DHS and XSBN were 181.5, 360.9, 536.2 and -320.0 g·C·m<sup>-2</sup>·a<sup>-1</sup>, respectively. From CBS to DHS, the temperature and precipitation increased with the decrease in latitude. The ratio of  $N_{EE}/R_0$  increased with latitude, while  $R_0/G_{PP}$ , ecosystem light use efficiency ( $L_{UE}$ ), precipitation use efficiency and average daily  $G_{PP}$  decreased gradually. However, XSBN usually escaped such latitude trend probably because of the influence of the south-west monsoon climate which does not affect the other ecosystems. Long-term measurement and more research were necessary to understand the adaptation of forest ecosystems to climate change and to evaluate the ecosystem carbon balance due to the complexity of structure and function of forest ecosystems.

www.scichina.com    www.springerlink.com

**Keywords:** forest transect, carbon budget, ecosystem photosynthesis, ecosystem respiration, China-FLUX, eddy covariance.

The responses and adaptation of terrestrial ecosystem to global changing were the premise for understanding the interaction between ecosystem and atmosphere<sup>[1]</sup>. As a major component of terrestrial ecosystems, forests play an important role in mitigating global climate change, and the carbon processes and exchanges of forest ecosystems have received great attention in global carbon cycling research<sup>[2-6]</sup>. Recently, long-term and continuous measurement of carbon flux became possible due to the advancement in the eddy covariance technique (EC), which has been assumed as the standard method in flux measurement<sup>[7]</sup> and applied to tropical rainforests<sup>[8-10]</sup>, temperate forests<sup>[11,12]</sup> and boreal forests<sup>[4,13,14]</sup> to provide the necessary data for the evaluation of ecosystem carbon balance. However, there is great uncertainty and inconsistency among current research: long-term measurement and more analysis are necessary to evaluate the carbon sink/source status of different forest ecosystems and to explain the response and adaptation of forest ecosystem carbon processes to climatic change<sup>[1,6]</sup>.

As the link and intermedium that couples different spatial and temporal scales and an effective approach to understand the regional responses under global changing, the transect method utilized the comparative research of different typical ecosystems under the environmental gradient to understand the response and adaptation of ecosystem function and processes to climatic change<sup>[15]</sup>. In China, the plentiful terrestrial ecosystems and environmental gradients provide a unique scientific platform for studying carbon cycling. Along the North-South Transect of Eastern China (NSTEC), carbon, water and energy fluxes of four typical ecosystems were measured with eddy covariance in ChinaFLUX from 2002. The long-term flux measurements will help to not only evaluate the ecosystem carbon budget under different environments, but also to analyze the response of ecosystem carbon processes and mechanism to global change on a regional scale<sup>[15,16]</sup>.

From cold temperate forests to tropical rainforests, NSTEC includes different types of forests and such transect was driven by the water and heat gradient<sup>[15]</sup>. This unique forest landscape was formed under the influence of the Eastern Asian monsoon climate, such as the subtropical evergreen broadleaf forest near the tropic of cancer in China, while such region was usually covered by desert or grassland in other regions. This study on this forest transect will help us to understand and evaluate the responses and adaptation of forest ecosystems to the East Asian monsoon climate. However, most previous research only focused on single forest ecosystems<sup>[17-19]</sup>, and integrated research has not been reported<sup>[15]</sup>. In this study, the carbon flux data from ChinaFLUX was utilized to analyze (1) seasonal variation in carbon exchange of typical forest ecosystems along the transect, (2) the environmental controlling mechanism of carbon exchange and (3) the effect of water and heat gradients on the carbon budget.

## 1 Materials and method

### 1.1 Site description

From north to south, the North-South Transect of Eastern China (NSTEC), the 15th standard transect of IGBP, mainly includes temperate mixed forest, warm temperate deciduous broadleaf forests, subtropical evergreen coniferous forests, subtropical evergreen broadleaf forests and tropical rainforests; and such transect was driven by the heat and water gradient. The CO<sub>2</sub>, H<sub>2</sub>O and energy fluxes of the Changbaishan temperate mixed forest (CBS), Qianyanzhou subtropical evergreen coniferous forest (QYZ), Dinghushan subtropical evergreen broadleaf forest (DHS) and Xishuangbanna tropical rainforest (XSBN) were measured continuously with eddy covariance technique from 2002. Basic information for each site is listed in Table 1; more detailed descriptions are provided in Liu *et al.*<sup>[17]</sup>, Guan *et al.*<sup>[18]</sup>, Zhou *et al.*<sup>[20]</sup> and Sha *et al.*<sup>[21]</sup>.

Table 1 Physical, vegetation and measurement feature of three forest sites

Site <sup>a)</sup>	CBS	QYZ	DHS	XSBN
Location	41°29'N, 128°05'E	26°44'N, 115°04'E	23°10'N, 101°12'E	21°30'N, 101°21'E
Topography	flat terrain	hilly region	hilly region	valley
Elevation /m	736	100	300	750
Mean Daytime air temperature (°C)	4.0	17.9	21.1	21.5
Precipitation/mm	695	1,485	1,956	1,493
Soil type	dark brown soil	red soil	lateritic red soil yellow soil	lateritic red soil
Canopy height (m)	26	11	15	36
LAI (m <sup>2</sup> ·m <sup>-2</sup> )	5.0 <sup>d</sup>	3.6	4.0	6.0
Dominant species	<i>Pinus koraiensis</i> , <i>Tilia amurensis</i> , <i>Quercus mongolica</i> , etc	<i>Pinus elliotii</i> , <i>Pinus massoniana</i> , <i>Cunninghamia lanceolata</i> , etc	<i>Cleistocalyx operculatus</i> , <i>Syzygium jambos</i> , <i>Castanopsis chinensis</i> , etc	<i>Pometia tomentosa</i> , <i>Terminalia myriocarpa</i> , <i>Barringtonia macrostachya</i> , <i>Garcinia cowa</i> , etc
Roughness height (m)	1.5	1.0	2.0	3.3
Height of EC (m)	40	39	27	48.8
Height of radiation/m	above canopy 32 below canopy 2	above canopy 42 below canopy 2	above canopy 36 below canopy 2	above canopy 48.8 below canopy 2
Precipitation (m)	70	42	36	70
Profiles of air temperature and humidity (m)	2.5, 8.0, 22.0, 26.0, 32.0, 50.0, 61.8	1.6, 7.6, 11.6, 15.6, 23.6, 31.6, 39.6	4.0, 9.0, 15.0, 21.0, 27.0, 31.0, 36.0	4.2, 16.3, 26.2, 36.5, 42.0, 48.8, 70
Soil temperature (m)	0.05	0.05	0.05	0.05
Soil moisture (m)	0.05, 0.20, 0.50	0.05, 0.20, 0.50	0.05, 0.20, 0.40	0.05, 0.20, 0.40

a) CBS, QYZ, DHS and XSBN indicate Changbaishan temperate mixed forest, Qianyanzhou subtropical evergreen coniferous forest, Dinghushan subtropical evergreen broadleaf forest and Xishuangbanna tropical rainforest, respectively.

## 1.2 Flux and routine meteorology measurement

Uniform open path eddy covariance system (OPEC) and observation methods were applied to measure the long-term and continuous CO<sub>2</sub>, H<sub>2</sub>O and energy fluxes between the biosphere and the atmosphere across different sites. 3D wind speed and temperature were measured with a 3D sonic anemometer (Model CSAT-3, Campbell Scientific Inc.) and the concentration of CO<sub>2</sub> and H<sub>2</sub>O were measured with an infrared gas analyzer (Model LI-7500, Licor Inc.). The raw 10 Hz data was collected and stored using a datalogger (Model CR5000, Campbell Scientific), and the 30 min flux data was calculated and exported to a computer. Routine meteorological factors such as radiation, temperature, precipitation and soil moisture, etc. were also measured with the same instruments at each site. The details of the measurement are also described in refs. [17, 18].

## 1.3 Flux calculation

1.3.1 CO<sub>2</sub> flux. Using the eddy covariance technique (EC), CO<sub>2</sub>, H<sub>2</sub>O and energy fluxes between the biosphere and the atmosphere were calculated with

measured wind pulse and scalar pulse<sup>[7]</sup>, and the CO<sub>2</sub> flux ( $F_c$ ) was calculated as

$$F_c = \overline{\rho w' c'}, \quad (1)$$

where  $\rho$  is the air density,  $c$  is the concentration of CO<sub>2</sub>, and  $w$  is the vertical wind speed. The over-bar indicates an averaging operation; the primes indicates the differences between instantaneous and mean values.

1.3.2 Canopy storage. For vegetation with a high canopy, as is typical of a forest, the net ecosystem exchange ( $N_{EE}$ ) is significantly influenced by canopy storage of CO<sub>2</sub> ( $F_s$ )<sup>[22]</sup>. Generally,  $F_s$  can be estimated through two approaches<sup>[14, 22]</sup>: the first approach is the CO<sub>2</sub> profile method in which the variation in concentration of CO<sub>2</sub> are measured within and above the canopy with a CO<sub>2</sub> profile system, and the second measures variations of CO<sub>2</sub> concentration at the measurement height. Because the CO<sub>2</sub> profile system was not available at DHS and XSBN,  $F_s$  was estimated with the second approach as in Hollinger *et al.*<sup>[22]</sup>,

$$F_s = \frac{\Delta c}{\Delta t} \cdot h, \quad (2)$$

where  $\Delta c$  is the change of CO<sub>2</sub> concentration between two continuous measurements,  $\Delta t$  is the time interval

between two continuous measurements ( $\Delta t$  is 1800 s in this study), and  $h$  is the measurement height.  $N_{EE}$  is calculated as

$$N_{EE} = F_c + F_s. \quad (3)$$

In this study, positive  $N_{EE}$  means that the vegetation sequestered  $\text{CO}_2$  from the atmosphere, while negative  $N_{EE}$  indicates that the ecosystem released  $\text{CO}_2$  to atmosphere.

1.3.3 Absorbed photosynthetic photon flux density. The absorbed photosynthetic photon flux density ( $Q_a$ ) was estimated as in Griffis *et al.*<sup>[14]</sup>,

$$Q_a = (1 - \eta) Q_p (1 - e^{-kLAI}), \quad (4)$$

where  $k$  is the extinction coefficient ( $k$  equals 0.5, 0.4, 0.4 and 0.5 for CBS, QYZ, DHS and XSBN, respectively),  $\eta$  is the canopy albedo of photosynthetic radiation ( $\eta$  equals 0.03, 0.04, 0.03 and 0.03),  $Q_p$  is incident the photosynthetic photon flux density, and LAI is the canopy leaf area index, estimated as,

$$LAI = -\frac{1}{k} \ln \left( \frac{Q_{p,b}}{Q_{p,a}} \right), \quad (5)$$

where  $Q_{p,b}$  and  $Q_{p,a}$  are the photosynthetic photon flux density measured below and above the canopy, respectively.

#### 1.4 Data processing

1.4.1 Coordinate rotation and WPL conversion. 3D coordinate rotation was applied to force the vertical wind speed to be zero and reduced the effect of topography<sup>[23]</sup>.  $\text{CO}_2$  concentration as measured by the infrared gas analyzer is the molar density rather than the molar ratio; thus, this measurement is affected by variation in air temperature, atmospheric pressure, and humidity<sup>[24]</sup>. In order to remove the influences of the variation in heat and water, the WPL conversion was applied after the coordinate rotation.

1.4.2 Data filtering. In order to obtain the true flux data representing the interaction between vegetation and atmosphere and to reduce noise, the raw data were filtered using the following steps: (i) data collected during rain was eliminated, (ii) the flux threshold was set to be  $[-3, 3]$  and eliminated the apparent spikes, (iii) according to the relationship between nighttime flux and friction wind speed ( $u^*$ ), the thresholds of  $u^*$  were identified as 0.1 for XSBN, and 0.2  $\text{m s}^{-1}$  for

CBS, QYZ and DHS, respectively<sup>[18,19]</sup>, and the nighttime flux data with  $u^*$  lower than the threshold were removed, and (iv) data that exceeded the  $\text{mean} \pm 1.96\sigma$  were removed. After data filtering, the available daytime data were 83%, 82%, 73% and 76%, while the nighttime data were only 34%, 30%, 34% and 15%, respectively.

1.4.3 Gap filling. Continuous data was necessary for the evaluation of the carbon budget with the eddy covariance technique, but data gaps were inevitable due to instrument failure, calibration and bad weather. The common methods for gap filling include mean daily variation (MDV), nonlinear regression, look-up table and neural network methods. In this study, the nonlinear regression method was applied to fill the data gaps. Short-time ( $< 2$  h) gaps were interpolated, while long-term daytime gaps were filled by inserting with the Michaelis-Menten model<sup>[25]</sup> using a time window of 30 days,

$$N_{EE} = \frac{\alpha Q_p P_{\max}}{\alpha Q_p + P_{\max}} - R_d, \quad (6)$$

where  $\alpha$  is the ecosystem photosynthetic photon yield ( $\text{mg CO}_2 \mu\text{mol}^{-1} \text{ photon}$ ),  $P_{\max}$  is the maximum photosynthetic rate ( $\text{mg CO}_2 \text{ m}^{-2} \cdot \text{s}^{-1}$ ),  $R_d$  is the daytime ecosystem respiration ( $\text{mg CO}_2 \text{ m}^{-2} \cdot \text{s}^{-1}$ ), and  $Q_p$  is the photosynthetic photon flux density ( $\mu\text{mol photon m}^{-2} \cdot \text{s}^{-1}$ ).

Nighttime gaps were inserted with the relationship between flux and temperature<sup>[25]</sup>,

$$N_{EE} = A e^{(BT)}, \quad (7)$$

where  $T$  is the soil or air temperature, both  $A$  and  $B$  are constants, and  $B = \ln(Q_{10}/10)$ ,  $Q_{10}$  is the sensitivity of respiration to temperature variation.

Short-time data gaps of routine meteorological factors ( $< 2$  h) were also interpolated, while long-term daytime gaps were inserted with gliding windows with window sizes of 14 and 7 for daytime and nighttime, respectively.

1.4.4 Estimation of ecosystem respiration and photosynthesis. Ecosystem respiration ( $R_e$ ) was usually estimated by two approaches. The first used the relationship between the nighttime flux and temperature as in equation (7). After the parameters were fitted, the relationship was scaled to the whole day to estimate the ecosystem respiration. The second used the rela-

tionship between daytime flux and  $Q_p$  as in equation (6), and after  $R_d$  was fitted, the ecosystem respiration could be estimated with equation (7). Ecosystem photosynthesis ( $G_{PP}$ ) was calculated as the sum of  $N_{EE}$  and  $R_e$ , i.e.

$$G_{PP} = N_{EE} + R_e. \quad (8)$$

With the processed and estimated data, the daily, monthly and annual  $R_e$ ,  $N_{EE}$ ,  $G_{PP}$  and routine meteorological factors were calculated. All data processing and calculations were completed with MATLAB (Math Works Inc., Natick, MA).

## 2 Results

### 2.1 Environmental factors

Compared to long-term records, the climate of each ecosystem was warmer and drier in 2003. The annual precipitation was particularly reduced, 37%, 43%, 34% and 23%, respectively (Figs. 1 and 2). At Changbaishan temperate mixed forest (CBS), precipitation and temperature demonstrate synchronous seasonal variation. During the growing season (April to September), the average daily temperature was 16°C and

the accumulated precipitation was 89% of annual precipitation. At Qianyanzhou subtropical evergreen coniferous forest (QYZ), a severe drought was observed during the summer. In July, the precipitation was low while the daily average temperature and VPD reached more than 30°C and 4 kPa, respectively, and the soil water content decreased to 0.1 m<sup>3</sup> m<sup>-3</sup> (Figs. 1 and 2). According to long term records, Dinghushan subtropical evergreen mixed forest (DHS) appeared to experience drought (from April to September) and wet seasons (from October to next March) in a year<sup>[26]</sup>. In 2003, the accumulated precipitation during the wet season accounted for 88% of annual accumulated precipitation. Under the influence of the Southwest monsoon climate, Xishangbanna tropical rainforest (XSBN) displayed an apparent fog-cool season (from November to next February), a dry-hot season (from March to April) and a wet-hot season (from May to October)<sup>[27]</sup>. During the three different seasons in 2003, the daily average temperatures were 18, 23 and 24°C, respectively, accumulated precipitation were 171, 147 and

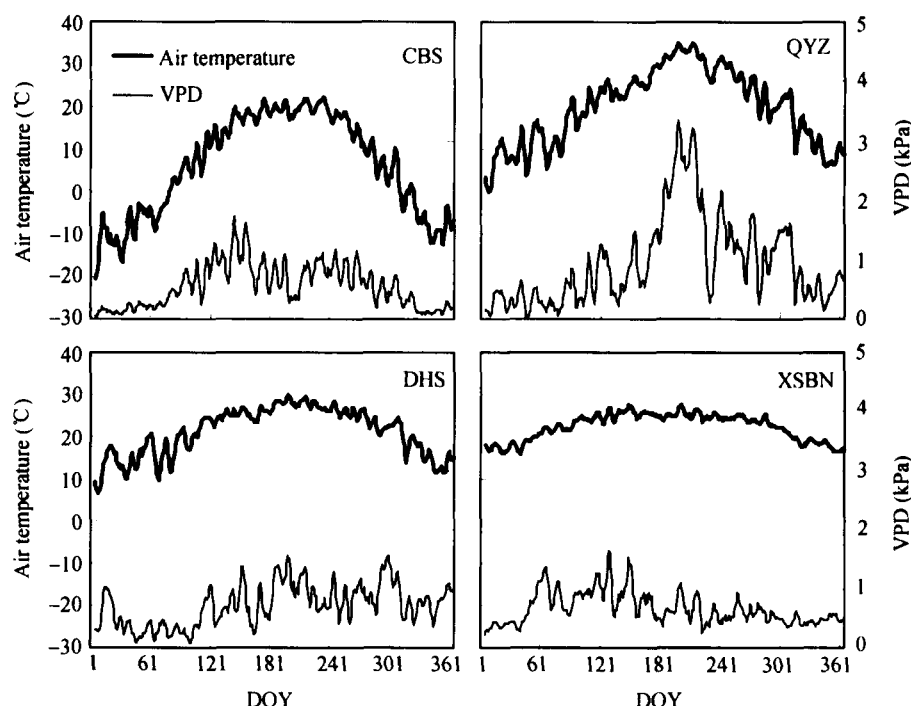


Fig. 1. Seasonal variations of daily average temperature (thick line) and VPD (thin line). In order to remove unnecessary noise, a running-mean filter with 5 windows was applied. CBS, QYZ, DHS and XSBN indicate Changbaishan temperate mixed forest, Qianyanzhou subtropical evergreen coniferous forest, Dinghushan subtropical evergreen broadleaf forest and Xishangbanna tropical rainforest, respectively.

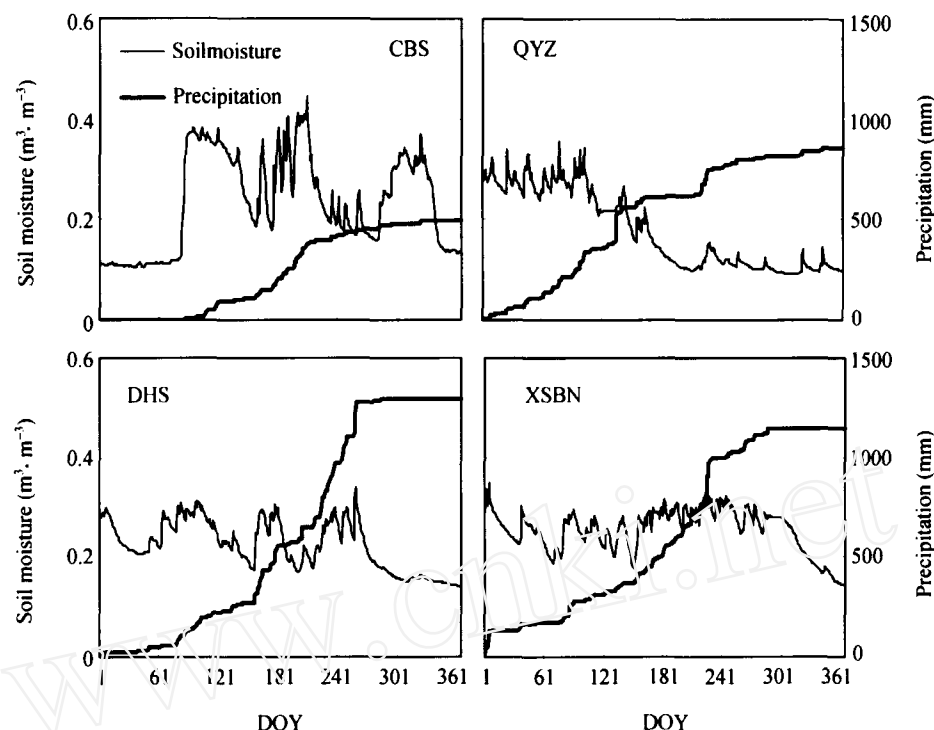


Fig. 2. Seasonal variation in daily average soil moisture (thick line) and daily accumulated precipitation (thin line). CBS, QYZ, DHS and XSBN indicate Changbaishan temperate mixed forest, Qianyanzhou subtropical evergreen coniferous forest, Dinghushan subtropical evergreen broadleaf forest and Xishaungbanna tropical rainforest, respectively.

832 mm, respectively, and the daily average VPD were 0.5, 0.9 and 0.7 kPa, respectively. Generally, the water and heat condition increased with decreasing latitude.

## 2.2 Ecosystem respiration and temperature

Ecosystem respiration ( $R_e$ ) was estimated with both daytime and nighttime flux (Fig 3); the estimated parameters and annual  $R_e$  are presented in table 2. During the estimation of nighttime flux, the data were block-averaged at 2°C intervals with at least 10 data points in each interval. The temperature selected for the estimation was different across the four ecosystems. For CBS and XSBN the soil temperature was selected, while the air temperature near the ground was selected for other two ecosystems. The selection of temperature with different heights was identified with the magnitude of relation coefficient between the nighttime flux and temperature, and this might reflect the different sources of ecosystem respiration. For CBS and XSBN the ecosystem respiration may mainly come from the soil respiration because of the old age and high content of soil organic matter<sup>[19]</sup>, whereas vegetation respiration may serve as the main source of

ecosystem respiration in the other two ecosystems. However more studies are needed to test such presumption.

Fig. 3 and Table 2 indicate that the two approaches yield different estimates of  $R_e$ . In CBS, QYZ and XSBN the estimated  $R_e$  with nighttime flux was higher than that with daytime flux, especially the difference attains more than 600 g·C·m<sup>-2</sup>·a<sup>-1</sup> at XSBN. Different turbulent intensity, flux fetch and plant ecophysiological responses might explain such differences in  $R_e$ . For example, during nighttime, the flux fetch would be much larger than that of daytime. In flux measurements, the nighttime flux could be assumed as the ecosystem respiration directly, so the estimated  $R_e$  with nighttime flux was adopted and analyzed in the following sections.

Table 2 shows that XSBN>CBS>QYZ>DHS for the temperature sensitivity of  $R_e$  ( $Q_{10}$ ) and annual  $R_e$ , while CBS>XSBN>QYZ>DHS for  $R_e$  under 15°C reference temperature ( $R_{ref,15}$ ). The annual  $R_e$  of CBS and QYZ are 1343 and 1280 g·C·m<sup>-2</sup>·a<sup>-1</sup>, respectively, which are comparable with the results of Yu *et al.*<sup>[19]</sup> (annual  $R_e$  estimated as 1268 and 1197 g·C·m<sup>-2</sup>·a<sup>-1</sup>,

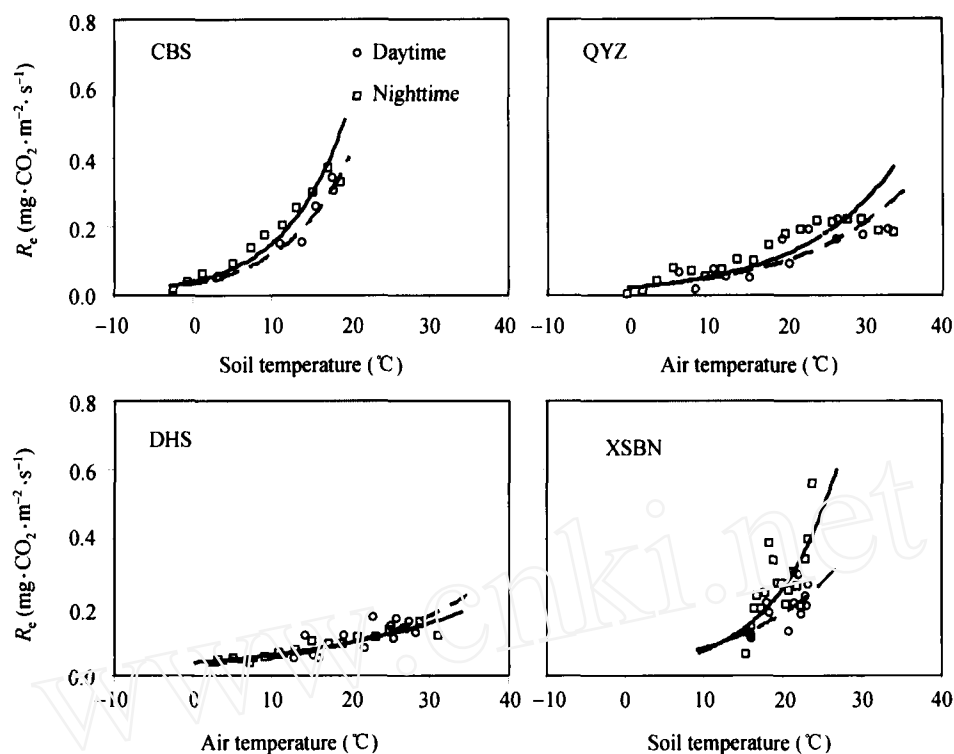


Fig. 3. Estimation of ecosystem respiration with nighttime and daytime flux data, respectively. The square and circular dots represent nighttime and daytime respiration respectively. The daytime respiration is estimated with equation (6) and 30 days gliding window. The nighttime respiration is the nighttime flux data and block averaged at 2 °C interval, and there are at least 10 data in each interval. The real and dash lines indicate the estimate respiration-temperature response curves with nighttime and daytime respiration, respectively.

Table 2 Ecosystem respiration estimated with daytime and nighttime flux data

Site		A	B	$Q_{10}$	$R_{ref,15}$ ( $\text{mg} \cdot \text{C} \cdot \text{m}^{-2} \cdot \text{s}^{-1}$ )	Annual $R_e$ ( $\text{g} \cdot \text{C} \cdot \text{m}^{-2} \cdot \text{a}^{-1}$ )
CBS	$R_{nf}$	0.0557	0.1065	2.90	0.275	1343.56
	$R_{df}$	0.0305	0.1319	3.74	0.220	1030.47
QYZ	$R_{nf}$	0.0516	0.0524	1.69	0.113	1280.36
	$R_{df}$	0.0401	0.0520	1.68	0.088	987.80
DHS	$R_{nf}$	0.0393	0.0472	1.60	0.080	918.94
	$R_{df}$	0.0362	0.0517	1.68	0.079	933.40
XSBN	$R_{nf}$	0.0272	0.1109	3.03	0.144	2246.72
	$R_{df}$	0.0398	0.0771	2.16	0.127	1634.47

A and B are constants;  $Q_{10}$  is the temperature sensitivity of ecosystem respiration which represents the relative variation of respiration when the temperature increase 10 °C;  $R_{ref,15}$  is the ecosystem respiration under reference temperature (15 °C);  $R_{nf}$  and  $R_{df}$  indicate the ecosystem respiration are estimated with nighttime and daytime flux, respectively.

respectively).

### 2.3 Responses of ecosystem carbon exchange to environment

Generally, ecosystem carbon exchange was determined by radiation, temperature and water condition<sup>[6,12]</sup>. In this study, the residual analysis method was applied to analyze the response of ecosystem carbon exchange to environmental factors (Fig. 4). Fig. 4(a)–(d) display the relationship between daily ac-

cumulated  $N_{EE}$  and radiation. At CBS there was an apparent growing and non-growing season during a year, while in the other three ecosystems growth could last the entire year, so only the data from growing season was selected at CBS.

The relationship between daily  $N_{EE}$  and radiation could be well described with Eq. (6) at CBS, QYZ and DHS (Fig. 4(a)–(c))<sup>[28]</sup>; however, this relationship could be described with linear or rectangular hyperbola, so a quadratic equation was used (Fig. 4(d)). At

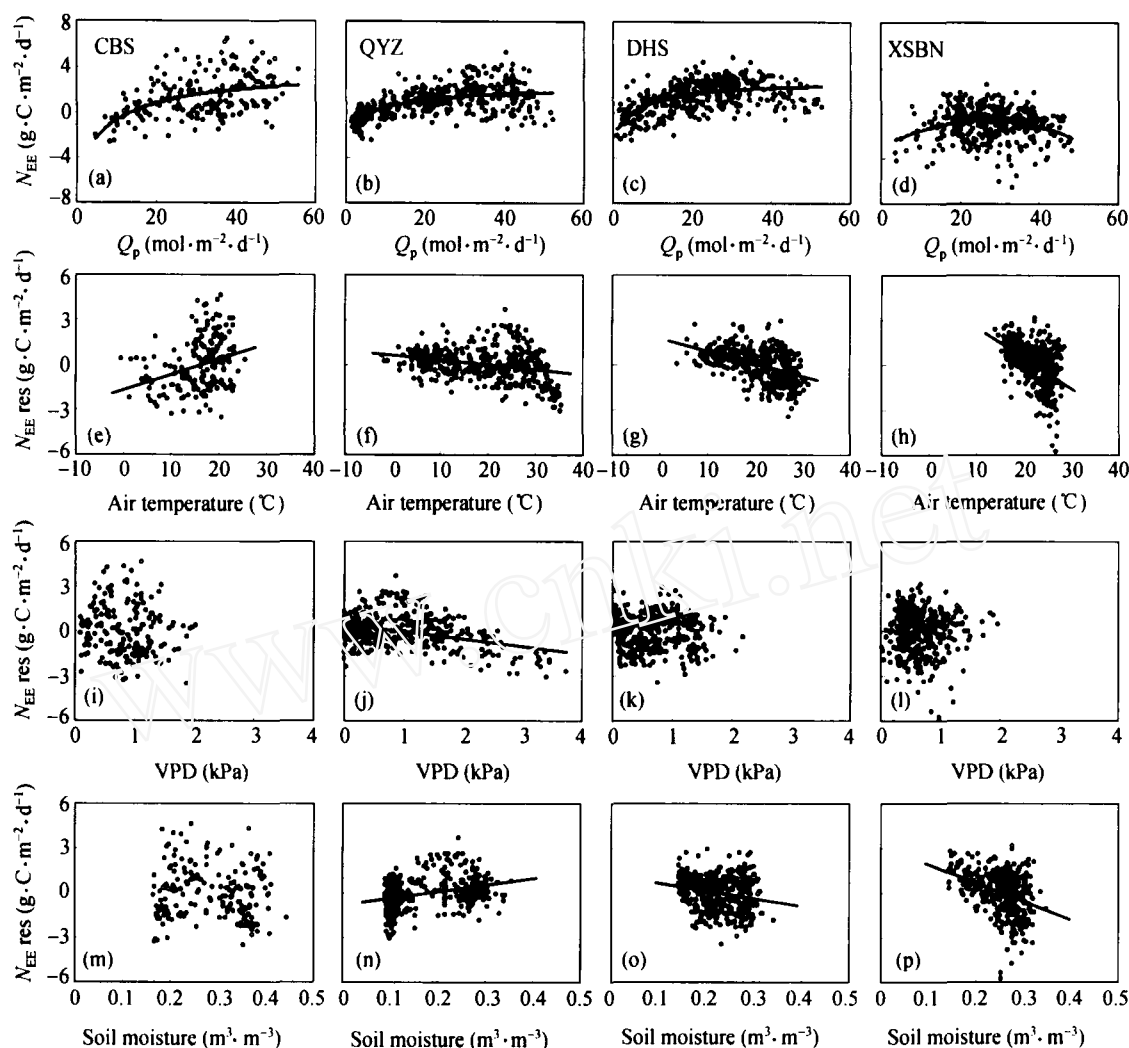


Fig. 4. The relationships between daily accumulated  $N_{EE}$  and residuals and environmental factors. Residual is the difference between  $N_{EE}$  and estimated  $N_{EE}$  with Eq. (6) or quadratic equation. (a)–(d) present the relationship between  $N_{EE}$  and radiation; (e)–(h) the  $NEE$  residuals and temperature; (i)–(l) the  $NEE$  residuals and VPD; (m)–(p) the  $NEE$  residuals and soil moisture. The real lines indicate the trend lines.

the scale of a day, the ecosystem photosynthetic photon yields ( $\alpha$ ) were 0.94, 0.61 and 0.74  $\text{g}\cdot\text{C}\cdot\mu\text{mol}^{-1}\cdot\text{photon}$  for CBS, QYZ and DHS, respectively, the ecosystem maximum photosynthetic rates ( $P_{\max}$ ) were 9.07, 4.45 and 5.09  $\text{g}\cdot\text{C}\cdot\text{m}^{-2}\cdot\text{s}^{-1}$ , and ecosystem daytime respiration rates ( $R_d$ ) were 5.34, 2.14 and 2.15  $\text{g}\cdot\text{C}\cdot\text{m}^{-2}\cdot\text{s}^{-1}$ , respectively. Clearly the potential photosynthetic capacity of CBS during the growing season was higher than that of the other ecosystems, while the respiration rate was also high.

Fig. 4(e)–(l) present the relationship between the residual and temperature, VPD and soil moisture. Residual was calculated as the difference between measured  $N_{EE}$  and estimated  $N_{EE}$  with Eq. (6) or a quadratic

equation, and the positive (negative) residual represented the high (low) efficiency of the ecosystem to sequester carbon under a given amount of radiation<sup>[29]</sup>. The relationship between residual and temperature are presented in Fig. 4(e)–(h). The residual of CBS increases linearly with temperature, while the residuals decrease for the other three ecosystems; the decrease of residual at QYZ became apparent when the temperature was higher than 30°C. Water vapor deficit (VPD) and soil moisture reflected the ecosystem water condition. The residual of CBS was not affected by VPD (Fig. 4(i)) or soil moisture (Fig. 4(m)), while the residuals of DHS and XSBN decreased with the improvement of soil moisture (Fig. 4(o) and 4(p)). This



indicated that no apparent drought was observed in CBS, DHS and XSBN. However, the residual of QYZ decreased with VPD and increased with the improvement of soil moisture rapidly due to the influence of severe drought during summer (Fig. 4(j) and 4(n)).

#### 2.4 Seasonal variations of ecosystem carbon exchange

Seasonal variation in ecosystem photosynthetic parameters,  $\alpha$ ,  $P_{\max}$  and  $R_d$  are presented in Fig. 5; these parameters were estimated with 30 min flux data with Eq. (6). Photosynthetic parameters of CBS displayed apparent single peak curves, with the maximum values appearing in June; these maxima were  $0.0041 \text{ mg} \cdot \text{CO}_2 \cdot \mu\text{mol}^{-1} \cdot \text{photon}^{-1}$ ,  $1.40 \text{ mg} \cdot \text{CO}_2 \cdot \text{m}^{-2} \cdot \text{s}^{-1}$  and  $0.34 \text{ mg} \cdot \text{CO}_2 \cdot \text{m}^{-2} \cdot \text{s}^{-1}$  for  $\alpha$ ,  $P_{\max}$  and  $R_d$ , respectively. Compared to CBS, seasonal variation in  $\alpha$  for QYZ, DHS and XSBN was not apparent. However,  $P_{\max}$  for QYZ, DHS and XSBN displayed seasonal variation comparable to CBS with maxima of 1.57, 1.18 and  $1.77 \text{ mg} \cdot \text{CO}_2 \cdot \text{m}^{-2} \cdot \text{s}^{-1}$ , respectively. During the summer,  $P_{\max}$  of QYZ, DHS and XSBN decreased due to different reasons. At QYZ, the decrease of  $P_{\max}$  resulted from the influence of severe drought. Insufficient radiation resulted from the excessive precipitation and fog during the wet season, perhaps accounting for the decrease in  $P_{\max}$  at DHS and XSBN.  $R_d$  of each ecosystem appeared similar seasonal variations as temperature (Fig. 1) and the maximum  $R_d$  increased as  $\text{DHS} < \text{QYZ} < \text{XSBN} < \text{CBS}$ .

Seasonal variation in  $N_{\text{EE}}$ ,  $R_e$  and  $G_{\text{PP}}$  are presented in Fig. 6. The carbon exchange of CBS mainly occurred during April to September, while it occurred over the entire year for other three ecosystems. The maximum  $N_{\text{EE}}$  occurred in early summer because  $G_{\text{PP}}$  attained a maximum earlier than  $R_e$ . After the maximum  $N_{\text{EE}}$  decreased with the decline of  $G_{\text{PP}}$  and the increase of  $R_e$  from August. This variation is similar to that described for a boreal deciduous broadleaf forest<sup>[14]</sup>. Under the influences of summer drought,  $N_{\text{EE}}$  of QYZ decreased significantly because of the depression of  $G_{\text{PP}}$ . During the wet season at DHS, the  $G_{\text{PP}}$  was depressed due to insufficient radiation resulting from the excessive rainfall and frequent fog.  $R_e$  also remained high under the higher temperature, while both  $G_{\text{PP}}$  and  $R_e$  were lower in drought season. As a result,

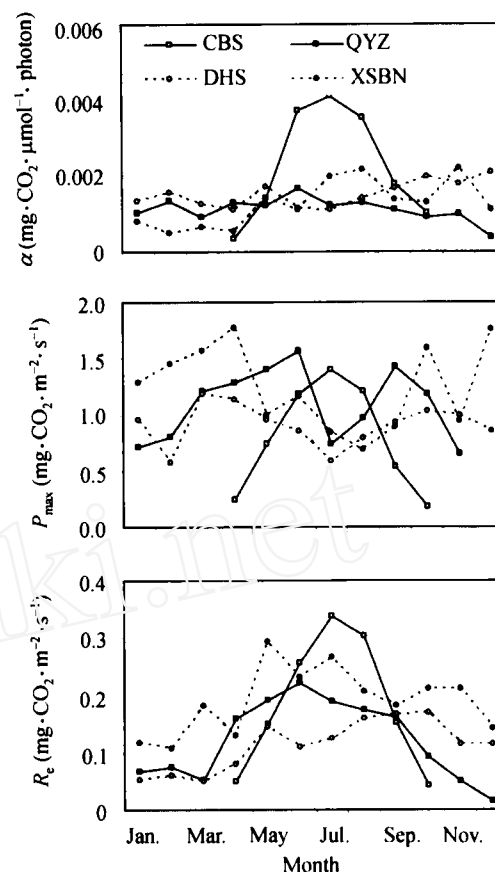


Fig. 5. The seasonal variations of ecosystem photosynthetic parameters estimated with Equation (6).  $\alpha$  is the ecosystem photosynthetic photon yield,  $P_{\max}$  is the ecosystem maximum photosynthetic rate, and  $R_d$  is the ecosystem daytime respiration.

seasonal variation in  $N_{\text{EE}}$  was relative flat and appeared to be a continuous carbon sink throughout the year. XSBN appeared to be a carbon sink during the fog-cool season, changing to carbon neutral status in the dry-hot season. However, such ecosystem became a moderate carbon source due to the depression of  $G_{\text{PP}}$  and increase of  $R_e$  under the humid and warm climate in the wet-hot season.

Seasonal variation in carbon budgets are presented with monthly ratio of  $G_{\text{PP}}/R_e$  in Fig. 7.  $G_{\text{PP}}/R_e < 1.0$ , indicates that the ecosystem  $G_{\text{PP}}$  was lower than  $R_e$ , and that the ecosystem is a carbon source.  $G_{\text{PP}}/R_e = 1.0$ , indicates carbon balance, i.e. the  $\text{CO}_2$  sequestered by  $G_{\text{PP}}$  was totally respired by  $R_e$ .  $G_{\text{PP}}/R_e > 1.0$  indicates that the ecosystem is a carbon sink<sup>[30]</sup>. Fig. 7 shows that seasonal variation in  $G_{\text{PP}}/R_e$  of CBS is similar to that of temperature (Fig. 1), and the ecosystem appeared to be the carbon sink during May to August, with the maximum ratio occurring in June. Although

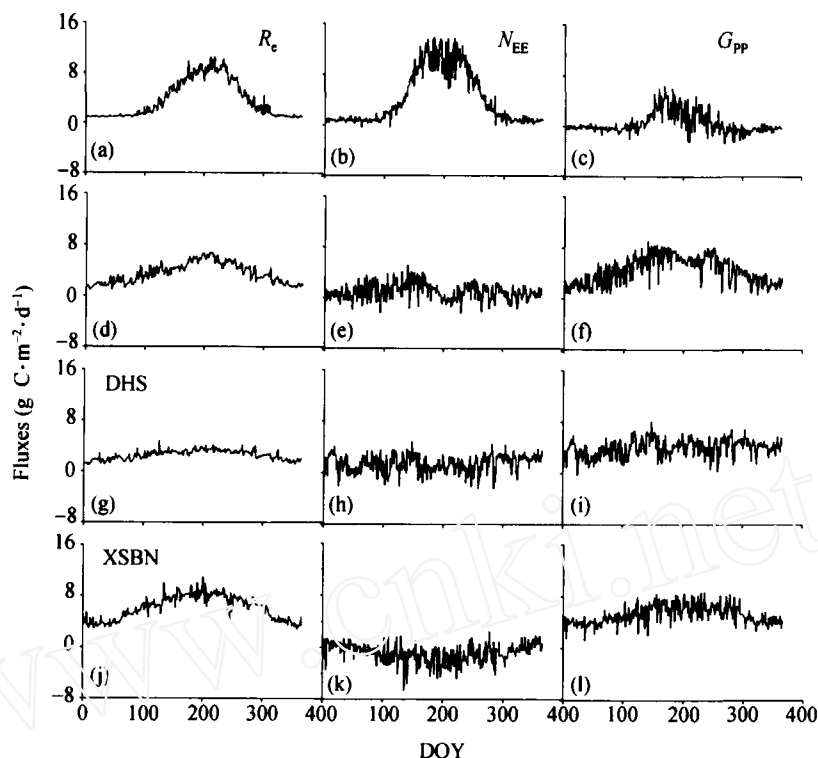


Fig. 6. Seasonal variation in  $N_{EE}$ ,  $R_e$  and  $G_{PP}$ .  $N_{EE}$  as calculated with the flux data filtered with  $u^*$ . The missing daytime data were filled with Equation (6) using a time window of 30 days, the missing nighttime data are filled with Eq. (7).  $R_e$  is estimated by the nighttime flux data with Eq. (7), and  $G_{PP} = N_{EE} + R_e$ .

QYZ appeared to be a carbon sink in every month, the ecosystem became nearly carbon balanced under the influence of summer drought in July. DHS appeared to be a continuous carbon sink for the entire year, especially in January and December when the  $G_{PP}$  was twice as large as  $R_e$ . At XSBN, nearly every monthly  $G_{PP}/R_e$  was lower than 1.0 except during the fog-cool season. The annual  $R_e/G_{PP}$  were 81%, 78%, 63% and 116% for CBS, QYZ, DHS and XSBN, respectively.

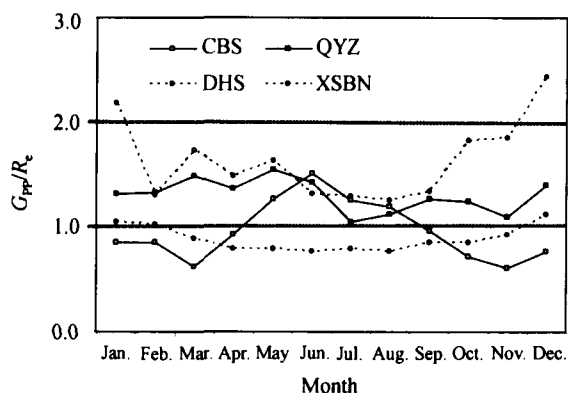


Fig. 7. Seasonal variation of  $G_{PP}/R_e$ . Each dot represents the ratio between monthly  $G_{PP}$  and  $R_e$ . The ratio  $G_{PP}/R_e > 1.0$ ,  $= 1.0$  and  $< 1.0$  indicates the ecosystem appears to be the carbon sink, carbon neutral and carbon source, respectively.

## 2.5 Annual carbon balances

The annual carbon budgets of CBS, QYZ, DHS and XSBN are presented in table 3.  $R_e$  was estimated with nighttime flux data, and  $G_{PP} = N_{EE} + R_e$ . In 2003, annual  $N_{EE}$  of CBS, QYZ, DHS and XSBN were 181.5, 360.9, 536.2 and  $-320.8 \text{ g} \cdot \text{C} \cdot \text{m}^{-2} \cdot \text{a}^{-1}$ , respectively.

Energy balance closure, which is usually represented by the ratio of available energy (solar radiation + soil heat flux + canopy heat storage) and turbulent energy (latent heat flux + sensible heat flux), could reflect the energy budget of the ecosystem<sup>[31]</sup>. Energy balance has been often utilized to evaluate the flux data quality<sup>[31]</sup> and correct the annual  $N_{EE}$ <sup>[14]</sup>. A former study indicated that the energy balance at CBS, QYZ, DHS and XSBN are 83%, 77%, 82% and 58% in 2003, respectively<sup>[32]</sup>. In this study annual carbon exchange was corrected with energy balance directly. Table 3 shows that replacement of low  $u^*$  data at night reduces the raw flux totals substantially. The EBC correction increased daytime fluxes more than nighttime fluxes and resulted in greater  $N_{EE}$  because  $G_{PP}$  was significantly larger than daytime  $R_e$ , while the

Table 3 Ecosystem carbon balances ( $\text{g}\cdot\text{C}\cdot\text{m}^{-2}\cdot\text{a}^{-1}$ )

Site	$R_e$		$G_{PP}$			$N_{EE}$	
	EBC	N-EBC	EBC	N-EBC	RAW	EBC	N-EBC
CBS	1618.7	1343.6	1837.4	1525.1	391.4	218.7	181.5
QYZ	1662.8	1280.4	2131.5	1641.3	687.6	468.7	360.9
DHS	1120.7	918.9	1774.6	1455.1	741.3	653.9	536.2
XSBN	3873.7	2246.7	3320.5	1925.9	120.2	-553.2	-320.8

EBC, Energy balance closure corrected flux values with the nighttime flux data filtered with  $u^*$ ; N-EBC, non-energy balance closure corrected flux values the nighttime flux data filtered with  $u^*$ ; RAW, non-energy balance closure corrected with low  $u^*$  nighttime observations included.  $R_e$  are derived from the nighttime flux data.  $G_{PP}$  is estimated as the sum of  $N_{EE}$  and  $R_e$ .

annual  $N_{EE}$  at XSBN become more negative because the  $G_{PP}$  was lower than  $R_e$ . EBC- and  $u^*$ -corrected annual  $N_{EE}$  were 218.7, 468.9, 653.9 and -553.2  $\text{g}\cdot\text{C}\cdot\text{m}^{-2}\cdot\text{a}^{-1}$  for CBS, QYZ, DHS and XSBN, respectively. The validity of the EBC method should be evaluated further<sup>[16]</sup>.

### 3 Discussion

#### 3.1 Compare to other forest ecosystems

Table 4 presents the carbon budgets of different forest ecosystems. The annual  $N_{EE}$  of CBS was within the range of variation of similar ecosystems. Compared to higher latitude coniferous forest ecosystems, annual  $N_{EE}$  of QYZ was similar to that of Le Bray forest. The annual  $N_{EE}$  of DHS was lower than that of Manaus and higher than that of Rond. However, XSBN appeared to be a moderate carbon source in 2003, while the other rainforest ecosystems in South America were carbon sinks.

#### 3.2 Influence of phenology on carbon budget

Ecosystem carbon budget was influenced significantly by phenology<sup>[7,14,30]</sup>. For the temperate forest ecosystem, the temperature determined the length of growing season and the amplitude of carbon exchange<sup>[14,30]</sup>. In 2003, ecosystem  $R_e$ ,  $N_{EE}$  and  $G_{PP}$  of CBS displayed similar seasonal variation to that of temperature; canopy development (LAI) was also influenced by temperature (Fig. 8(a)).

The ecosystem photosynthesis ( $G_{PP}$ ) was influenced by temperature and leaf area via enzyme activity during the photosynthesis and photosynthetic area. In order to quantify the respective contribution of temperature and leaf area to  $G_{PP}$ , a simple method was applied. First, the amplitude of LAI during the winter was assumed to be the background LAI ( $LAI_b$ ); this was

about  $1.5 \text{ m}^2\cdot\text{m}^{-2}$ . Second, the  $G_{PP}$  of per unit LAI ( $G_{PPa}$ ) was calculated as the ratio of  $G_{PP}$  and the corresponding LAI. Third, the contribution of temperature to  $G_{PP}$  ( $G_{PPt}$ ) was estimated as  $LAI_b$  times  $G_{PPa}$ ; the difference between  $G_{PP}$  and  $G_{PPt}$  indicates the contribution from leaf area ( $G_{PP,LAI}$ ). Fig. 8(b), shows that both  $G_{PPt}$  and  $G_{PP,LAI}$  increase with temperature, but the increase of  $G_{PP,LAI}$  is much more rapid (Fig. 8(b)). According to the fitted curves, the contributions from temperature and leaf area were 615 and 910  $\text{g}\cdot\text{C}\cdot\text{m}^{-2}$ , respectively.

Two temperature thresholds significantly affected the seasonal variation in carbon exchange and leaf area at CBS. The ecosystem  $R_e$  and  $G_{PP}$  become active after the temperature exceeded the threshold of  $0^\circ\text{C}$  in the middle March, when leaf area also increases and new buds and leaves flush out. Carbon exchange became inactive below the threshold of  $0^\circ\text{C}$  in late October (Fig. 8(a)). When temperatures exceeded  $10^\circ\text{C}$  on the 3rd of April, however, carbon exchange increased rapidly, then decreased quickly after the temperature dropped below  $10^\circ\text{C}$  in late September. Seasonal variation in LAI also displayed a similar response to temperature (Fig. 8(a)). Fig. 9 shows that  $R_e$ ,  $N_{EE}$ ,  $G_{PP}$ , and LAI increase rapidly after temperature exceeds  $10^\circ\text{C}$ , while a small increase occurs when temperature increases from  $0^\circ\text{C}$  to  $10^\circ\text{C}$ .

Under the influence of subtropical high pressure, QYZ experienced severe drought from late June to August due to low precipitation and high temperature.  $G_{PP}$  decreased significantly during the drought period (Figs. 6 and 7). In May and June, when no apparent drought was observed, the monthly  $N_{EE}$  were 68.8 and 62.2  $\text{g}\cdot\text{C}\cdot\text{m}^{-2}\cdot\text{mon}^{-1}$ , respectively. However, monthly  $N_{EE}$  decreased to 8.6 and 19.8  $\text{g}\cdot\text{C}\cdot\text{m}^{-2}\cdot\text{mon}^{-1}$  in July and August, respectively. With the apparent rainfall in

Table 4 Comparison of  $N_{EE}$  among different forest ecosystems

Site	$N_{EE}$ ( $\text{g}\cdot\text{C}\cdot\text{m}^{-2}\cdot\text{a}^{-1}$ )	Vegetation type	Latitude
Camp Borden	60–240 <sup>a)</sup>	temperate mixed forest	44°19'N
Collelongo, Selva Piana	210–660 <sup>a)</sup>	temperate mixed forest	41°50'N
Takayama	120–214 <sup>a)</sup>	temperate mixed forest	36°08'N
Tomakomai	293 <sup>1)</sup>	temperate mixed forest	42°44'N
Harvard Forest	120–303.1 <sup>a)</sup>	temperate mixed forest	42°32'N
Howland Forest	210–321.9 <sup>a)</sup>	temperate mixed forest	45°20'N
Sask., SSA Old Aspen	122 <sup>[14]</sup>	temperate mixed forest	53°63'N
CBS	181	temperate mixed forest	42°40'N
Sask., SSA Old Black Spruce	35–68 <sup>1)</sup> [14]	boreal evergreen coniferous forest	53°59'N
Sask., SSA Old Jack Pine	78 <sup>[14]</sup>	boreal evergreen coniferous forest	53°54'N
Le Bray, Bordeaux	372.5–575 <sup>a)</sup>	boreal evergreen coniferous forest	44°43'N
Bayreuth	76.3 <sup>a)</sup>	boreal evergreen coniferous forest	50°09'N
Reno/Ritten Bolzano	450 <sup>a)</sup>	boreal evergreen coniferous forest	46°35'N
Niwot Ridge Forest	57.6–152.5 <sup>a)</sup>	boreal evergreen coniferous forest	40°01'N
Wind River Crane	476.2 <sup>a)</sup>	boreal evergreen coniferous forest	45°49'N
QYZ	360.9	subtropical evergreen coniferous forest	26°75'N
Rond., Rebio Jaru Ji Parana	102 <sup>a)</sup>	tropical evergreen broadleaf forest	10°04'S
Manaus	601.7 <sup>a)</sup>	tropical evergreen broadleaf forest	02°36'S
DHS	536.2	subtropical evergreen broadleaf forest	23°17'N
La Selva	–0.05–792 <sup>[10]</sup>	rainforest	10°26'N
Ducke	220 <sup>[33]</sup>	rainforest	02°57'S
Jarú	100 <sup>[34]</sup>	rainforest	10°04'S
Cuieriras	590 <sup>[8]</sup>	rainforest	02°35'S
XSBN	–320	tropical seasonal rainforest	21°96'N

a) Data source: <http://www.fluxnet.ornl.gov/fluxnet/nee.cfm>; The positive  $N_{EE}$  indicates the  $\text{CO}_2$  into the ecosystem, while the negative indicates the  $\text{CO}_2$  release from ecosystem.

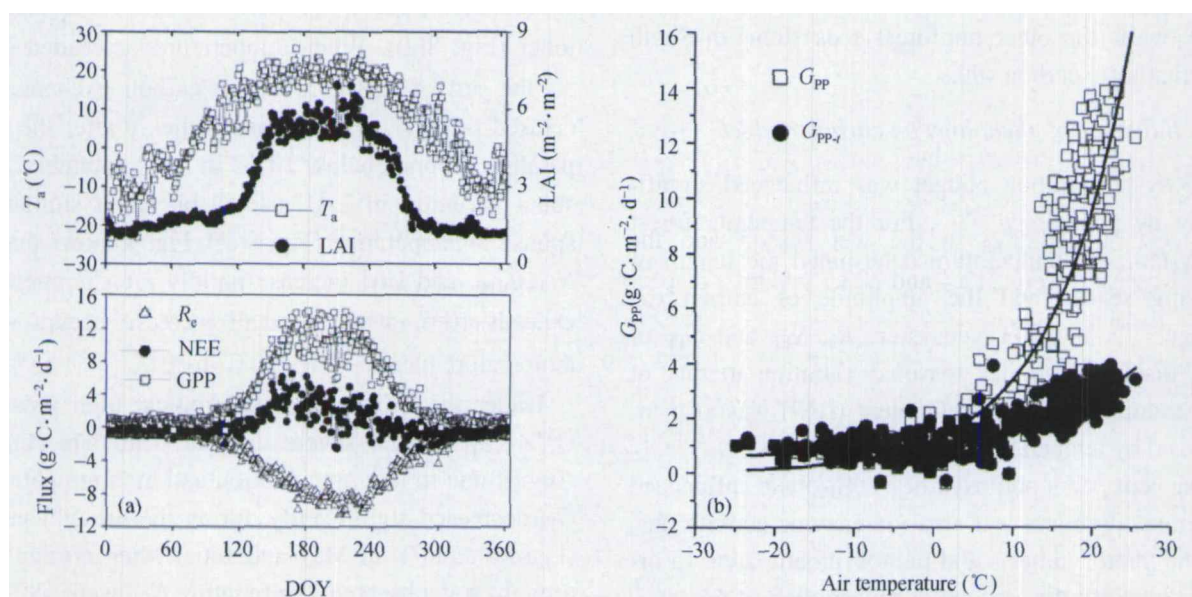


Fig. 8. (a) The coordinated seasonal variations of ecosystem  $R_e$ ,  $N_{EE}$ ,  $G_{PP}$ , LAI and air temperature ( $T_a$ ) at CBS. In order to display the seasonal variations clearly, the negative  $G_{PP}$  means ecosystem sequesters  $\text{CO}_2$  from atmosphere. (b) The respective contribution of temperature and leaf area (LAI) to ecosystem photosynthesis ( $G_{PP}$ ). The positive  $G_{PP}$  means ecosystem sequesters  $\text{CO}_2$  from atmosphere.  $G_{PP,t}$  indicates the contribution of temperature, and the difference between  $G_{PP}$  and  $G_{PP,t}$  indicates the contribution of leaf area. The real lines are trend lines.

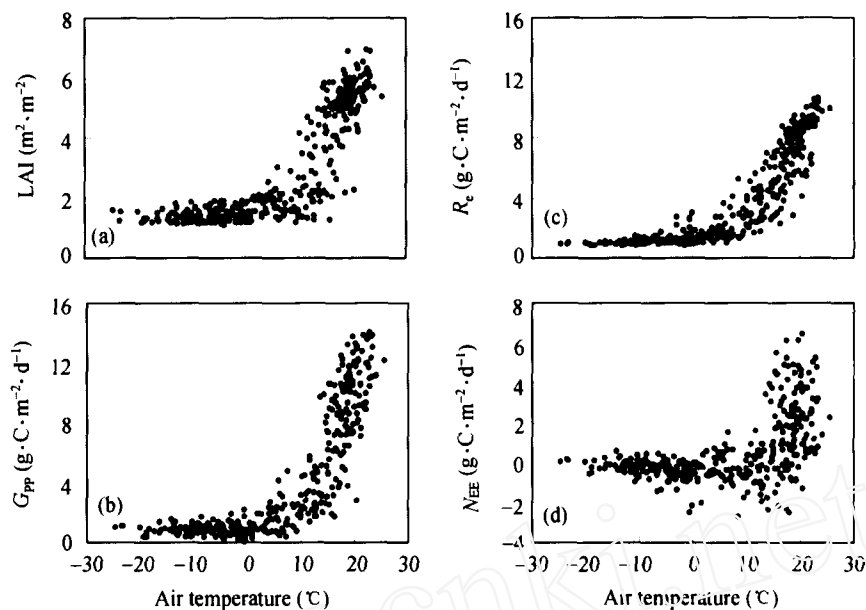


Fig. 9. The relationship between average daily temperature and LAI (a),  $G_{PP}$  (b),  $R_e$  (c) and  $N_{EE}$  (d).

September, monthly  $N_{EE}$  recovered to  $37.8 \text{ g} \cdot \text{C} \cdot \text{m}^{-2} \cdot \text{mon}^{-1}$ .

According to long term records at DHS, the wet season lasts from April to September, while the drought season lasts from October to March of the following year. In 2003, the accumulated precipitation was 150.7 and 1148.7 mm in the drought and wet season, respectively (Table 5). During the wet season, the average daily  $G_{PP}$  was only  $0.4 \text{ g} \cdot \text{C} \cdot \text{m}^{-2} \cdot \text{d}^{-1}$  higher than that of the drought season, while average daily  $R_d$  increased  $1.0 \text{ g} \cdot \text{C} \cdot \text{m}^{-2} \cdot \text{d}^{-1}$ , then  $N_{EE}$  decreased  $0.6 \text{ g} \cdot \text{C} \cdot \text{m}^{-2} \cdot \text{d}^{-1}$ . The ecosystem photosynthetic parameters also showed that the  $P_{max}$  of the wet season was lower than that of the drought season, while  $R_e$  was higher. The accumulated  $N_{EE}$  in the wet season and the drought season were 212.4 and  $323.7 \text{ g} \cdot \text{C} \cdot \text{m}^{-2}$ , respectively.

Distinct characteristics of carbon exchange during different seasons were also observed at XSBN (Fig. 6 and Table 5). Compared to the drought-hot season and the wet-hot season, the decrease of  $R_e$  was more apparent than  $G_{PP}$  during the fog-cool season, so the ecosystem appeared to be a carbon sink. Although  $G_{PP}$  increased with the improvement of temperature, the increment of  $G_{PP}$  was lower than  $R_e$  during the drought-hot and wet-hot seasons (Table 5). Particularly during the wet-hot season, the plentiful rainfall

and resultant frequent fog were not favorable to  $G_{PP}$ , while  $R_e$  increased with the improvement of water and heat. Influenced by  $G_{PP}$  and  $R_e$ , ecosystem carbon balance changed from a carbon sink to a carbon source during the drought-hot and wet-hot seasons. Vourlitis *et al.*<sup>[9]</sup> and Loescher *et al.*<sup>[10]</sup> indicated that a tropical rainforest in Brazil and Central America appeared to be a moderate carbon sink due to the improvement of water and temperature during wet season, while Goulden *et al.*<sup>[35]</sup> found that  $R_e$  was lower due to the slow decomposition of soil organic matter during the drought season, so  $N_{EE}$  was higher than that of wet season, and such variation was also displayed at XSBN.

### 3.3 Latitudinal trend of ecosystem carbon exchange

Along with the latitude, the environmental factors showed apparent latitudinal variations and such variations influenced the ecosystem carbon exchange significantly (Table 6). Fig. 6 presents the environmental factors and parameters that relate to ecosystem carbon exchange; only the data for growing season (April to September) was selected for CBS. Along the latitudinal gradient from CBS to DHS,  $R_e/G_{PP}$  decreased while  $N_{EE}/G_{PP}$  increased as temperature and precipitation increased.  $N_{EE}/R_e$  also increased with the decrease in latitude, and this result is similar to that observed in European temperate and boreal forests<sup>[4]</sup>.

Table 5 The ecosystem exchange and environmental factors during different seasons at DHS and XSBN.

	Period	$T_a$ (°C)	VPD (kPa)	$M$ ( $\text{m}^3 \text{m}^{-3}$ )	$P$ (mm)	$R_e$ ( $\text{g} \cdot \text{C} \cdot \text{m}^{-2} \cdot \text{d}^{-1}$ )	$N_{EE}$ ( $\text{g} \cdot \text{C} \cdot \text{m}^{-2} \cdot \text{d}^{-1}$ )	$G_{PP}$ ( $\text{g} \cdot \text{C} \cdot \text{m}^{-2} \cdot \text{d}^{-1}$ )	$\alpha$ ( $\text{mg} \cdot \mu\text{mol}^{-1}$ )	$P_{\max}$ ( $\text{mg} \cdot \text{m}^{-2} \cdot \text{s}^{-1}$ )	$R_d$ ( $\text{mg} \cdot \text{m}^{-2} \cdot \text{s}^{-1}$ )
Dinghushan subtropical evergreen mixed forest											
Drought season	10-3	16.6	0.63	0.20	150.7	2.0	1.8	3.8	0.0015	0.93	0.088
Wet season	4-9	25.6	0.80	0.24	1148.7	3.0	1.2	4.2	0.0015	0.76	0.129
XSBN tropical seasonal rainforest											
Fog-cool season	11-2	18.3	0.48	0.23	170.6	4.0	0.1	4.1	0.0018	0.85	0.182
Drought-warm season	3-4	23.2	0.93	0.24	147.1	5.7	-0.9	4.8	0.0006	1.64	1.154
Wet-warm season	5-10	24.8	0.69	0.28	831.5	7.7	-1.5	6.2	0.0017	0.90	0.240

$T_a$  is air temperature; VPD is water vapor deficit;  $M$  is soil moisture;  $P$  is annual precipitation. The precipitation is the accumulative value, while the other environmental factors are the average daily value during the corresponding season.  $R_e$ ,  $N_{EE}$  and  $G_{PP}$  are the average daily value during the corresponding season.  $\alpha$ ,  $P_{\max}$  and  $R_d$  are estimated during the corresponding season respectively.

Table 6 The environmental factors and carbon exchange parameters

	CBS	QYZ	DHS	XSBN
Air temperature	16.16	19.76	21.12	22.35
VPD	0.84	0.94	0.71	0.66
Soil moisture	0.23	0.18	0.22	0.26
$Q_p$	5774.38	3877.16	8342.82	10108.44
$Q_a$	4924.43	7001.65	6828.92	9558.25
$P$	439.3	854.9	1299.4	1149.2
$G_{PP}/R_e$	1.13	1.28	1.58	0.86
$G_{PP}/N_{EE}$	8.44	4.56	2.73	-5.98
$G_{PP}/Q_a$	0.31	0.24	0.21	0.20
$N_{EE}/D$	0.99	0.99	1.47	-0.88
$G_{PP}/D$	8.37	4.51	4.01	5.26
$R_e/D$	7.38	3.52	2.54	6.14
$G_{PP}/P$	3.49	1.93	1.13	1.67

Temperature (°C), VPD (kPa) and Soil moisture ( $\text{m}^3 \cdot \text{m}^{-3}$ ) are average daily value;  $Q_p$  ( $\text{mol} \cdot \text{photon} \cdot \text{m}^{-2}$ ),  $Q_a$  ( $\text{mol} \cdot \text{photon} \cdot \text{m}^{-2}$ ) and precipitation (mm) are annual accumulation.  $N_{EE}$ ,  $R_e$  and  $G_{PP}$  are annual accumulation ( $\text{g} \cdot \text{C} \cdot \text{m}^{-2} \cdot \text{a}^{-1}$ ).  $D$  indicates the days during the growing season. In CBS, the growing season is from April to September, and  $D=183$ , while for the other three ecosystems,  $D=365$ .

Although average daily  $NEE$  ( $N_{EE}/D$ ) decreased with decreasing latitude, light use efficiency ( $G_{PP}/Q_a$ ), precipitation use efficiency ( $G_{PP}/P$ ) and average daily  $G_{PP}$  ( $G_{PP}/D$ ) increased gradually. Such variation might reflect the fact that limited water and heat were used with high efficiency during the limited growing season at CBS. However, both the sensitivity of respiration to temperature ( $Q_{10}$ ) and average daily  $R_e$  ( $R_e/D$ ) of CBS were higher than that of QYZ and DHS (Table 6), and this may relate to the old age (about 200 years) of, and plentiful organic matter in, the soil<sup>[19]</sup>.

The parameters mentioned above at XSBN typically does not follow the latitudinal trends described above. A possible explanation is that ecosystems such as XSBN located in the southwest of China are mainly influenced by the Southwest monsoon. Another possible explanation is that the data presented here may be biased by short-term phenomena since data were only

analyzed for a single year. Long-term measurements may be necessary to confirm these results.

#### 4 Conclusions

Seasonal variation and their responses to the environment of Changbaishan temperate mixed forest (CBS), Qianyanzhou subtropical evergreen coniferous forest (QYZ), Dinghushan subtropical evergreen mixed forest (DHS) and Xishuanbanna tropical seasonal rainforest (XSBN) along the North-South Transect of Eastern China were studied with the eddy covariance technique. The results showed that,

(1) The ecosystem carbon budget at CBS appeared to be coordinated with seasonal variation in temperature and leaf area (LAI); the contribution from leaf area was about  $910 \text{ g} \cdot \text{C} \cdot \text{m}^{-2}$ , higher than that of the direct effect of temperature,  $615 \text{ g} \cdot \text{C} \cdot \text{m}^{-2}$ . Two tem-

perature thresholds were observed during the seasonal variation of carbon exchange. The first, 0 °C, determined the length of the growth season, and the other, 10 °C, affected the magnitude of carbon exchange. During the summer, QYZ experienced severe drought due to low precipitation and high temperature; during this period  $N_{EE}$  decreased significantly due to a decrease in  $G_{PP}$ .  $N_{EE}$  of both DHS and XSBN was higher in the drought season and lower in the wet season; the ecosystem carbon balance changed from carbon sink to source at XSBN during the transition between the fog-cool season and the wet season. The depression of  $G_{PP}$  resulting from excessive humid and the increase in  $R_e$  with the temperature during the wet season probably explained such  $N_{EE}$  variations at DHS and XSBN.

(2) At CBS, QYZ and XSBN, the estimated annual  $R_e$  with nighttime flux data was higher than that estimated with daytime flux data. With respect to temperature sensitivity of ecosystem respiration ( $Q_{10}$ ) and annual  $R_e$ , XSBN > CBS > QYZ > DHS; the average daily  $R_e$  of CBS during the growing season was the highest.

(3) In 2003, CBS, QYZ and DHS appeared to be carbon sinks, and annual  $N_{EE}$  were 181.5, 360.9 and 536.2  $\text{g}\cdot\text{C}\cdot\text{m}^{-2}\cdot\text{a}^{-1}$ , respectively. XSBN was a moderate carbon source of 320.8  $\text{g}\cdot\text{C}\cdot\text{m}^{-2}\cdot\text{a}^{-1}$ .

(4) From CBS to DHS, both the temperature and precipitation increased with the decrease in latitude. Along this latitudinal gradient, ecosystem  $R_e/G_{PP}$  decreased gradually, from 88% at CBS to 78% at QYZ to 63% at DHS, while  $N_{EE}/R_e$  increased with the decrease in latitude. Average daily  $G_{PP}$ , ecosystem light use efficiency and precipitation use efficiency decreased with the decrease in latitude. However, XSBN typically did not follow this latitudinal trend. In this study, only one year was analyzed, while not only the structure and role of terrestrial ecosystem were complexity, but also the responses and adaptation of different ecosystems to climatic change were different, so long term data and more work were necessary to understand such processes and evaluate the carbon budget.

**Acknowledgements** This study was supported by the Knowledge Innovation Project of the Chinese Academy of

Sciences (Grant No. KZCX1-SW-01-01A) and the National Key Research and Development Program (Grant No. 2002CB412501).

## References

- 1 Global Carbon Project. Science Framework and Implementation. Earth System Science Partnership (IGBP, IHDP, WCRP, DIVERSITAS) Report No.1: Global Carbon Project Report No. 1 Canberra, 2003, 22—23
- 2 Dixon R K, Brown S, Houghton R A, et al. Carbon pools and flux of global forest ecosystem. *Science*, 1994, 263: 185—190
- 3 Malhi Y, Baldocchi D D, Jarvis P G. The carbon balance of tropical, temperate and boreal forest. *Plant, Cell and Environment*, 1999, 22: 715—740
- 4 Valentini R, Matteucci G, Dolman A J, et al. Respiration as the main determinant of carbon balance in European forests. *Nature*, 2000, 404: 861—865
- 5 Barford C C, Wofsy S C, Goulden M L, et al. Factors controlling long- and short-term sequestration atmospheric  $\text{CO}_2$  in a mid-latitude forest. *Science*, 2001, 294: 1688—1691
- 6 Law B E, Falge E, Gu L, et al. Environmental controls over carbon dioxide and water vapor exchange of terrestrial vegetation. *Agricultural and Forest Meteorology*, 2002, 113: 97—120
- 7 Baldocchi D D, Falge E, Gu L H, et al. FLUXNET: A new tool to study the temporal and spatial variability of ecosystem-scale carbon dioxide, water vapor and energy flux densities. *Bull Am Meteorol Soc*, 2001, 82: 2415—2434
- 8 Malhi Y, Nobre A D, Grace J, et al. Carbon dioxide transfer over a Central Amazonian rain forest. *Journal of Geophysical Research*, 1998, 103: 31, 593—31, 513, 612
- 9 Voulitis G L, Filho N P, Hayashi M M S, et al. Seasonal variations in the net ecosystem  $\text{CO}_2$  exchange of a mature Amazonian transitional tropical forest. *Functional Ecology*, 2001, 15: 388—395
- 10 Loescher H W, Oberbauer S F, Gholz H L, et al. Environmental controls on net ecosystem-level carbon exchange and productivity in a Central American tropical wet forest. *Global Change Biology*, 2003, 9: 396—412
- 11 Greco S, Baldocchi D D. Seasonal variation of  $\text{CO}_2$  and water vapor exchange rates over a temperate deciduous forest. *Global Change Biology*, 1996, 2: 183—197
- 12 Aubinet M, Chermanne B, Vandenhaute M, et al. Long-term carbon dioxide exchange above a mixed forest in the Belgian Ardennes. *Agriculture and Forest Meteorology*, 2001, 108: 293—315
- 13 Baldocchi D D, Vogel C A, Hall B. Seasonal variation of carbon dioxide exchange rates above and below a boreal jack pine forest. *Agriculture and Forest Meteorology*, 1997, 83: 147—170
- 14 Griffis T J, Black T A, Morgenstern K, et al. Ecophysiological controls on the carbon balances of three southern boreal forests. *Agriculture and Forest Meteorology*, 2003, 117: 53—71
- 15 Yu G-R, Zhang L-M, Sun X M, et al. Advances in carbon flux observation and research in Asia. *Sci China Ser D-Earth Sci*, 2005, 48 (Supp. 1): 1—16

- 16 Baldocchi D D. Assessing the eddy covariance technique for evaluating carbon dioxide exchange rates of ecosystems: Past, present and future. *Global Biology Change*, 2003, 9: 479—492
- 17 Liu Y F, Song X, Yu G-R, et al. Seasonal variation of CO<sub>2</sub> flux and its environmental factors in evergreen coniferous plantation. *Sci China Ser D-Earth Sci*, 2005, 48 (Supp I): 123—133
- 18 Guan D X, Wu J B, Yu G-R, et al. Meteorological Control on CO<sub>2</sub> flux above broad-leaved Korean pine forest in Changbai mountains. *Sci China Ser D-Earth Sci*, 2005, 48 (Supp. I): 116—122
- 19 Yu G-R, Wen X F, Li Q K, et al. Seasonal patterns and environmental control of ecosystem respiration in subtropical and temperate forests in China. *Sci China Ser D-Earth Sci*, 2005, 48 (Supp. I): 93—105
- 20 Zhou C Y, Zhou G Y, Zhang D Q, et al. CO<sub>2</sub> efflux from different forest soils and impact factors in Dinghu Mountain, China. *Sci China Ser D-Earth Sci*, 2005, 48 (Supp. I): 198—206
- 21 Sha L Q, Zhen Z, Tang J W, et al. Soil respiration in a tropical seasonal rain forest in Xishuangbanna, SW China. *Sci China Ser D-Earth Sci*, 2005, 48 (Supp. I): 189—197
- 22 Hollinger D Y, Kelliher F M, Byers J N, et al. Carbon dioxide exchange between an undisturbed old-growth temperate forest and the atmosphere. *Ecology*, 1994, 75: 134—150
- 23 Wilczak J M, Oncley S P, Stage S A. Sonic anemometer tilt correction algorithms. *Bound-Lay Meteorology*, 2001, 99: 127—150
- 24 Webb E K, Pearman G I, Leuning R. Correction of flux measurement for density effects due to heat and water vapour transfer. *Q J Roy Meteor Soc*, 1980, 106: 85—100
- 25 Falge E, Baldocchi D, Olson R, et al. Gap filling strategies for defensible annual sums of net ecosystem exchange. *Agricultural and Forest Meteorology*, 2001, 107, 43—69
- 26 Yan J H, Zhou G Y, Zhang D Q, et al. Spatial and temporal variations of some hydrological factors in a climax forest ecosystem in the Dinghushan region. *Acta Ecologica Sinica*, 2003, 23(11): 2359—2366
- 27 Zhang K Y. The characteristics of south Yunan and preliminary analysis of its formation. *Acta Meteorologica Sinica*, 1966, 33: 210—230
- 28 Ruimy A, Jarvis P G, Baldocchi D D, et al. CO<sub>2</sub> fluxes over plant canopies and solar radiation: A review. *Advances in Ecological Research*, 1995, 26: 1—81
- 29 Aubinet M, Heinesch B, Longdoz B. Estimation of the carbon sequestration by a heterogeneous forest: night flux corrections, heterogeneity of the site and inter-annual variability. *Global Change Biology*, 2002, 8: 1053—1071
- 30 Falge E, Baldocchi D, Tenhunen J, et al. Seasonality of ecosystem respiration and gross primary production as derived from FLUXNET measurements. *Agriculture and Forest Meteorology*, 2002, 113: 53—74
- 31 Wilson, K, Goldstein, A, Falge, E, et al., Energy balance closure at FLUXNET sites. *Agricultural and Forest Meteorology*, 2002, 223—243
- 32 Li Z Q, Yu G-R, Wen X F, et al. Energy balance closure at ChinaFLUX sites. *Sci China Ser D-Earth Sci*, 2005, 48 (Supp. I): 51—62
- 33 Fan S-M, Wofsy S C, Bakwin P S, et al. Atmosphere-biosphere exchange of CO<sub>2</sub> and O<sub>3</sub> in the central Amazon forest. *Journal of Geophysical Research*, 1990, 25: 12851—16864
- 34 Grace J, Lloyd J, McIntyre J, et al. Fluxes of carbon dioxide and water vapor over an undisturbed tropical rainforest in south-west Amazonia. *Global Change Biology*, 1995, 1: 1—12
- 35 Goulden M L, Miller S D, Da Rocha H R, et al. Diel and seasonal patterns of tropical forest CO<sub>2</sub> exchange. *Ecological Applications*, 2004, 14(4, Supplement): S42—S54